Reactivity of Pt and Pt−Sn Alloy Surfaces Probed by Activation of C_5−C_8 Cycloalkanes via Electron-Induced Dissociation (EID) of Multilayers

Yi-Li Tsai and Bruce E. Koel*

Department of Chemistry, University of Southern California, Los Angeles, California 90089-0482

Received July 3, 1997. In Final Form: January 22, 1998

The surface chemistry of cycloalkanes and cycloalkyl intermediates on Pt−Sn alloys is important to the function of selective hydrocarbon conversion catalysts, yet very little is known about this chemistry because cycloalkane decomposition is strongly suppressed under UHV conditions on Pt−Sn alloys and there are few other clean sources of these intermediates. Low-energy, electron-induced dissociation (EID) in multilayers of saturated hydrocarbons produces rather cleanly reactive intermediates formed by the selective cleavage of one C−H bond. This method was used to activate C_5−C_8 cycloalkane multilayers and prepare monolayer coverages of cycloalkyl species on Pt(111) and two well-defined Pt−Sn alloy surfaces—the p(2×2)-Sn/Pt(111) and ($\sqrt{3}\times\sqrt{3}$)R30°Sn/Pt(111) surface alloys formed by vapor deposition of Sn on a Pt(111) substrate. EID of the multilayers and subsequent thermal reactions of the intermediates on these surfaces were investigated by temperature-programmed desorption (TPD), Auger electron spectroscopy (AES), and low-energy electron diffraction (LEED). Adsorbed cycloalkyl species dehydrogenate facilely on both alloy surfaces, but alloying with Sn weakens the bonding to the surface of the cycloalkenes formed and strongly suppresses cycloalkene dehydrogenation. This chemistry leads to a much higher selectivity for the evolution of gas-phase cycloalkenes from the dehydrogenation of cycloalkyl intermediates compared to that on Pt(111).

1. Introduction

Hydrocarbon conversion, specifically catalytic re-forming, is one of the most important industrial applications of catalysis. In the re-forming process, saturated hydrocarbons are converted to aromatic hydrocarbons and linear alkanes are converted to branched alkanes as selectively as possible because of the high antiknock quality of aromatic and branched hydrocarbons. Model re-forming reactions have been extensively studied under high-pressure conditions,[1,2] and much is known about the overall reaction kinetics. However, a molecular level understanding of these reactions is still not available, partly because of the difficulty of preparing and characterizing the chemistry of adsorbed alkyl intermediates in these reactions.

Brian Bent, a friend and inspiration to many of us, was well-known for his work on generating, isolating, and reacting surface intermediates on metal single crystals in a vacuum and explaining how this chemistry mimics important aspects of heterogeneous catalysis. Not long ago, he wrote a beautiful review article summarizing some of his many contributions to this field.[3]

Several different methods have been used to synthesize hydrocarbon intermediates on surfaces: radical sources,[4,5] thermal dissociation of alkyl iodides,[6−9] photodissociation of alkyl halides,[10−12] collision of high-energy molecular beams with surfaces,[13,14] dissociation of adsorbed molecules by helium ions,[15] H atom addition or abstraction by atomic hydrogen,[16,17] electron-induced dissociation (EID) of physisorbed molecules,[18−21] and high-pressure reactions in an attached reaction cell.[22−26] All of these methods have severe limitations. Hyperthermal molecular beam methods may not be selective when using large molecules. High-pressure reaction studies suffer from a lack of control for producing a single, or a desired, adsorbate. Cross-sections for H atom abstraction are very similar before and after abstraction occurs, and thus additional incident H atoms can continue to form additional dehydrogenated products. Using alkyl iodides as dissociation precursors has the ever-present problem

* To whom correspondence should be addressed.

(1) Davis, S. M.; Somorjai, G. A. In *The Chemical Physics of Solid Surfaces and Heterogeneous Catalysis*; King, D. A., Woodruff, D. P., Eds.; Elsevier: Amsterdam, 1984; Vol. 4, Chapter 7.
(2) Sinfelt, J. H. In *Catalysis, Science and Technology*; Anderson, J. R., Boudart, M., Eds.; Springer-Verlag: Berlin, 1981; Vol. 1, Chapter 5.
(3) Bent, B. E. *Chem. Rev.* **1996**, *96*, 1361.
(4) Peng, X. D.; Viswanathan, R.; Smudde, G. H., Jr.; Stair, P. C. *Rev. Sci. Instrum.* **1992**, *63*, 3930.
(5) Chiang, C. M.; Bent, B. E. *Surf. Sci.* **1992**, *279*, 79.
(6) Zaera, F. *J. Phys. Chem.* **1990**, *94*, 8350.
(7) Zhou, X.-L.; White, J. M. *J. Phys. Chem.* **1991**, *95*, 5575.
(8) Hugenschmidt, M. B.; Domagala, M. E.; Campbell, C. T. *Surf. Sci.* **1992**, *275*, 121.
(9) Chiang, C. M.; Wentzlaff, T. H.; Bent, B. E. *J. Phys. Chem.* **1992**, *96*, 1836.
(10) Lloyd, K. G.; Roop, B.; Campion, A.; White, J. M. *Surf. Sci.* **1989**, *214*, 227.
(11) Zhou, X.-L.; White, J. M. *Surf. Sci.* **1991**, *241*, 244.
(12) Zhou, Y.; Feng, W. M.; Henderson, M. A.; Roop B.; White, J. M. *J. Am. Chem. Soc.* **1988**, *110*, 4447.
(13) Ceyer, S. T. *Langmuir* **1990**, *6*, 82.
(14) Lee, M. B.; Yang, Q. Y.; Ceyer, S. T. *J. Chem. Phys.* **1987**, *87*, 2724.
(15) Beckerle, J. D.; Yang, Q. Y.; Johnson, A. D.; Ceyer, S. T. *J. Chem. Phys.* **1987**, *86*, 7236.
(16) Xi, M.; Bent, B. E. *J. Phys. Chem.* **1993**, *97*, 4167.
(17) Xi, M.; Bent, B. E. *J. Vac. Sci. Technol.* **1992**, *B10*, 2440.
(18) Zhou, X.-L.; Castro, M. E.; White, J. M. *Surf. Sci.* **1990**, *238*, 215.
(19) Zhou, X.-L.; White, J. M. *J. Phys. Chem.* **1992**, *96*, 7703.
(20) Zhou, X.-L.; Schwaner, A. L.; White, J. M. *J. Am. Chem. Soc.* **1993**, *115*, 4309.
(21) White, J. M. *Langmuir* **1994**, *10*, 3946.
(22) Campbell, C. T. *Adv. Catal.* **1989**, *36*, 1.
(23) Rodriguez, J. A.; Goodman, D. W. *Surf. Sci. Rep.* **1991**, *14*, 1.
(24) Kahn, D. R.; Petersen, E. E.; Somorjai, G. A. *J. Catal.* **1974**, *34*, 294.
(25) Koel, B. E.; Bent, B. E.; Somorjai, G. A. *Surf. Sci.* **1984**, *146*, 211.
(26) Campbell, C. T.; Koel, B. E. *Surf. Sci.* **1987**, *183*, 100.

S0743-7463(97)00711-7 CCC: $15.00
Published on Web 02/27/1998

with coadsorbed iodine, which can dramatically influence the reaction on the surface. For example, the activation energy for vinyl coupling to form butadiene on Ag(111) is lowered from 15.2 to 6.3 kcal/mol by coadsorbed iodine.[20]

One of the most useful methods for preparing and characterizing hydrocarbon fragments on Group IB transition metals (Cu, Ag, Au) is EID. White[21] has reviewed this approach, concluding that for 10−50-eV incident electrons on physisorbed species "impact ionization leads to cleavage of one C−H bond and, with significant yield, a single hydrocarbon species characterized by a strong C−metal bond." Several examples, such as methyl and vinyl, can be given, but one of the nicest results is the synthesis and kinetic characterization of phenyl species from benzene adsorbed on Ag(111).[21] The selectivity in EID using low-energy electrons to dissociate monolayers[18−21] is unfortunately limited to weakly adsorbed molecules, and this also usually implies relatively unreactive surfaces such as Cu, Ag, and Au. This is simply because the metal substrate quenches excitations induced by low-energy electrons in cases of moderate and strong chemisorption, and EID of the precursor is no longer effectively self-limiting. In common practice, however, many of the most interesting systems include moderately or strongly bonded adsorbates.

Some time ago, we made a simple extension of the above approach that extends this method to reactive metal surfaces.[27,28] Instead of using monolayer coverage, we produce a multilayer. The additional layers are isolated from the substrate by the monolayer, and excitations induced by low-energy electrons have a prolonged lifetime which opens a dissociation pathway. These reactive fragments, after C−H bond cleavage, diffuse to the surface[29] and become adsorbed. Subsequent EID reactions of this strongly bound intermediate are greatly inhibited (by a factor exceeding 10^3) by strong quenching from the metal. If the hydrocarbon precursor in the multilayer is symmetrical, that is, contains only one type of C−H bond, then there is a large propensity for forming a single type of adsorbed intermediate. Our previous work[27,28] showed that we could produce an adsorbed cyclohexyl monolayer on Pt(111) via EID of cyclohexane multilayers.

We have recently investigated the adsorption and reaction of a series of cycloalkanes—cyclopropane (c-C_3H_6), cyclopentane (c-C_5H_{10}), cycloheptane (c-C_7H_{14}), and cyclooctane (c-C_8H_{16})—on Pt(111)[30] and two Pt−Sn alloys.[31] Cyclohexane (c-C_6H_{12}) was studied on these surfaces previously.[28] In all cases, thermal decomposition of the cycloalkanes is strongly suppressed on the Pt−Sn alloys, and in the particular case of cyclohexane, no thermal decomposition occurs under UHV conditions during TPD. To probe the subsequent chemistry of the dehydrogenation of cycloalkanes, we have used EID to activate cycloalkane multilayers to form monolayers of cycloalkyl species on Pt(111) and two ordered Pt−Sn surface alloys. A homologous series of cycloalkanes, C_5−C_8, were investigated. Cyclopentyl species have often been proposed as intermediates for dehydrocyclization reactions,[1,2] cyclohexyl is clearly involved in cyclohexane to benzene conversion,[28] and cycloheptyl and cyclooctyl species may be important in other re-forming reactions. Here, we have concentrated our attention on the desorption products, especially alkenes and aromatics, from dehydrogenation of cycloalkyl species on these three surfaces during TPD. Our goal is not to fully elucidate the decomposition mechanism and kinetics at this point but simply to survey and explore what is the effect of surface Sn on altering the Pt chemistry. These results show that alloyed Sn weaken alkenes and aromatic chemisorption and strongly suppresses dehydrogenation of unsaturated products, leading to improved selectivity for the evolution of alkenes and aromatics and decreased carbon formation compared to that on Pt(111).

2. Experimental Methods

These experiments were carried out in a stainless steel UHV chamber pumped by a 220 L/s ion pump, a Ti sublimation pump, and a 170 L/s turbomolecular pump with a base pressure of 2×10^{-10} Torr during experiments. This chamber was equipped with a double-pass cylindrical mirror analyzer (CMA) for Auger electron spectroscopy (AES), a four-grid optics for low-energy electron diffraction (LEED), a UTI model 100 C quadrupole mass spectrometer (QMS) for TPD, and an ion gun for Ar^+ ion sputtering. A stainless steel shield with an aperture of about 1-cm diameter covered the ionizer region of the QMS. To reduce (<60 nA) electron emission from the ionizer, two high-transparency stainless steel screens were used—one across the end of the ionizer grid (with a bias of −55 V) and one across the entrance aperture of the shield (at ground potential)—between the ionizer region and the sample.

A variable-energy electron gun (5−1000 eV, Kimball Physics, Model FRA-2x1-2) was used in these experiments. Low-energy EID was carried out using an incident electron beam energy of 50 eV with the sample grounded. The incident beam current was 1 μA, as measured with a sample bias of +225 V, impinging on the entire sample holder. The uniformity of the electron beam over the sample was checked by measurements using a faraday cup with a 1-mm-diameter hole. At the sample position (1.0 in. from the end of the electron gun), the maximum beam intensity was 0.29 μA/cm^2 and the beam fwhm was 9 mm in diameter, compared to the Pt(111) crystal diameter of 8 mm. The average electron flux on the crystal was ~0.24 μA/cm^2 or 1.5×10^{12} electrons/cm^2·s.

The Pt(111) single crystal (8-mm diameter) was cleaned by a standard procedure using 1-keV Ar^+ ion sputtering, annealing to 1000 K in a vacuum, heating to 800 K in 2×10^{-8} Torr O_2, and finally flashing to 1200 K in a vacuum. The cleanliness of the crystal was checked by AES and LEED prior to each experiment. Two well-defined Pt−Sn surface alloys, the p(2×2)Sn/Pt(111) and ($\sqrt{3}\times\sqrt{3}$)R30°Sn/Pt(111) alloys, with a stoichiometry of Pt_3Sn and Pt_2Sn, respectively, were prepared prior to each experiment by evaporation of 1−3 monolayers of Sn onto the Pt(111) surface and annealing to 1000 K for about 10 s depending on the particular alloy to be formed. The structure and composition of each preparation were confirmed by both LEED and the Sn(430)/Pt(237) AES peak-to-peak height ratio. For convenience, the p(2×2)Sn/Pt(111) and ($\sqrt{3}\times\sqrt{3}$)R30°Sn/Pt(111) surface alloys will be referred to as the (2×2) and $\sqrt{3}$ alloys throughout this paper. A schematic diagram of the two-dimensional structure of these surfaces is shown in Figure 1. Alloyed Sn is substituted into the topmost Pt(111) layer at Pt sites, producing a relatively flat surface, but with Sn atoms displaced, or "buckled", outward from the surface plane by 0.02 nm. These structures were first solved by using low-energy alkali ion scattering spectroscopy (ALISS)[32] and have now been confirmed independently by LEED I−V analysis[33] and X-ray photoelectron diffraction (XPD).[34]

The gas samples, cyclopentane (c-C_5H_{10}, Aldrich 95%), cyclohexane (c-C_6H_{12}, Aldrich 99%), cycloheptane (c-C_7H_{14}, Aldrich 98%), and cyclooctane (c-C_8H_{16}, Aldrich 99%), were used without further purification other than degassing by several freeze−pump−thaw cycles. All of the gas exposures were made by using a microcapillary array doser connected to the leak valve and given at a substrate temperature of 100 K or below.

(27) Xu, C.; Koel, B. E. *Surf. Sci.* **1993**, *292*, L803.
(28) Xu, C.; Tsai, Y.-L.; Koel, B. E. *J. Phys. Chem.* **1994**, *98*, 585.
(29) Tsai, Y.-L.; Koel, B. E. *J. Phys. Chem.* **1997**, *101*, 4781.
(30) Tsai, Y.-L.; Koel, B. E. In preparation.
(31) Tsai, Y.-L.; Koel, B. E. In preparation.
(32) Overbury, S. H.; Mullins, D. R.; Paffett, M. T.; Koel, B. E. *Surf. Sci.* **1991**, *254*, 45.
(33) Atrei, A.; Bardi, U.; Rovida, G.; Torrini, M.; Zanazzi, E.; Ross, P. N. *Phys. Rev.* **1992**, *B46*, 1649.
(34) Galeotti, M.; Atrei, A.; Bardi, U.; Rovida, G.; Torrini, M. *Surf. Sci.* **1994**, *313*, 349.

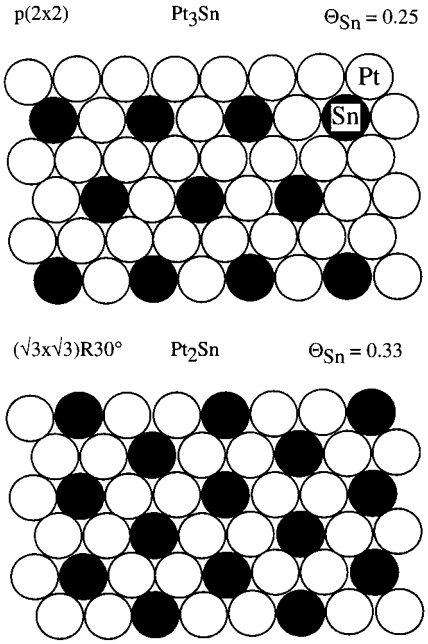

Figure 1. Schematic diagram of the structure of two Sn/Pt-(111) surface alloys. Top: Top view of the (2×2)Sn/Pt(111) surface alloy. Bottom: Top view of the $(\sqrt{3}\times\sqrt{3})$R30°Sn/Pt-(111) surface alloy. The 3D structure of these surfaces is nearly planar, but the Sn is buckled above the Pt surface plane by 0.22 Å.[32−34]

All of the EID experiments utilized an incident electron beam energy of 50 eV. EID of physisorbed hydrocarbons using a low fluence at this electron energy selectively activates and dissociates a single C−H bond via impact ionization and leads in the cases discussed herein to a chemisorbed monolayer containing predominately a single cycloalkyl species.[21,27] We used an average electron exposure in 300 s of 4.5 × 10^{14} electrons/cm^2. This electron exposure was sufficient to "saturate" the EID reactions, as confirmed by plotting the attenuation of the TPD area of the cycloalkane monolayer peak and the increase of H_2 TPD peak area as a function of electron exposure for 3-ML films of cyclohexane and cyclooctane on Pt(111) at 100 K. The *overall* reaction cross-section of these 3-ML cycloalkane films was about (2−8) × 10^{-15} cm^2, which is the same order of magnitude as that in our previous determination using nominally 55-eV electrons from the QMS ionizer.[27] Low-energy EID is sensitive to the adsorption character of the target species; the cross-section is at least 1000 times higher for physisorbed layers than for chemisorbed layers on Pt(111). It may also be sensitive to fairly small differences between the second layer and thicker layers. Ideally, we tried to obtain a condensed cycloalkane film with an equivalent coverage of 3 ML (calibrated by the molecular TPD monolayer peak area on the $\sqrt{3}$ alloy) for all of these molecules on these surfaces to ensure the effectiveness of the EID process for creating monolayers of cycloalkyl species. Some molecular desorption from the monolayer was often seen after EID of cycloalkane multilayers, which could possibly be due to using less than 3-ML (but always more than 2 ML) films but is more likely due to facile hydrogenation of cycloalkyl fragments during TPD. In either case, this only affects the exact amount but not the variety of EID products.

The TPD measurements were made with the sample placed 1 mm in front of the entrance aperture of the QMS shield, in line-of-sight with the QMS ionizer, and using a linear heating rate of 4 K s^{-1}. For all of the molecules and surfaces studied, with and without electron bombardment, we monitored signals during TPD at 2 (H_2); 15, 16 (CH_x); 26, 28, 30 (C_2H_x); 40, 42, 44 (C_3H_x); 52, 54, 56, 58 (C_4H_x); 66, 68, 70, 72 (C_5H_x); and 78 (benzene) amu. In addition, we monitored signals at larger masses for the larger cycloalkanes, as indicated below, and also checked at the appropriate masses to detect for dimerization products from C−C bond coupling of cycloalkyl groups on these surfaces. No dimerization product was ever detected in TPD.

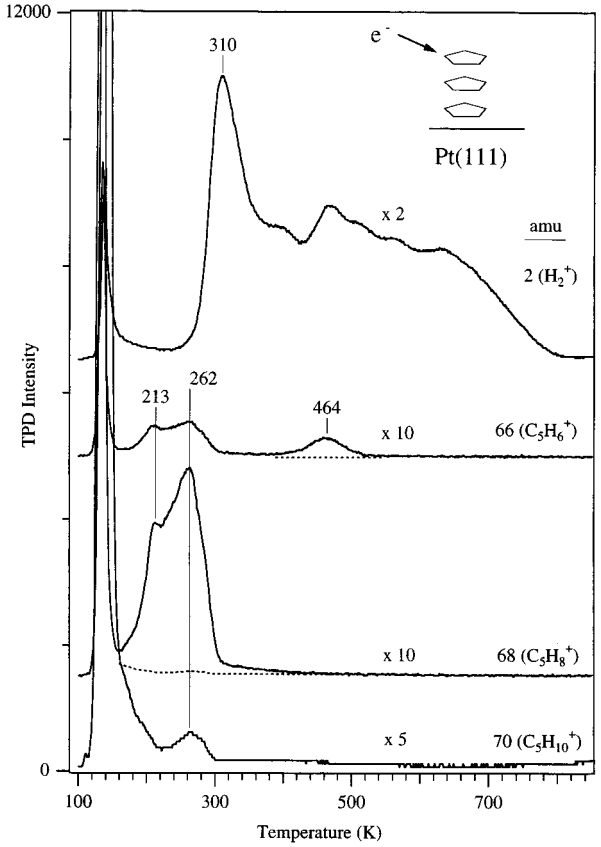

Figure 2. TPD spectra after EID of a 3-ML cyclopentane (c-C_5H_{10}) film on Pt(111) at 100 K. The dashed curve in this and all of the following figures indicates the contribution of cracking fragments from other molecules to the observed spectra.

The assignment of the hydrocarbon products desorbed during TPD is a difficult task, and we have not made a detailed study. Here we are mainly interested in trends in the relative yields and desorption temperatures of unsaturated product molecules. However, we can propose tentative assignments for the desorbed products on the basis of our previous studies on these surfaces. Alkenes and cycloalkenes, those molecules containing a single C=C bond, should desorb at 260−290 K on Pt(111), 210−270 K on the (2×2) alloy, and 170−210 K on the $\sqrt{3}$ alloy.[35,36] Dienes and cyclodienes, molecules containing two C=C bonds, may not desorb because of easy dehydrogenation, but adsorption energies can be reasonably estimated to be twice the di-σ-bond strength and desorption may occur at 520−570 K on Pt(111), 420−530 K on the (2×2) alloy, and 335−420 K on the $\sqrt{3}$ alloy.[37] Alkynes, molecules containing a single C≡C bond, should not desorb on Pt(111) because of its high reactivity but desorb at 300−510 K on the (2×2) alloy and 365 K on the $\sqrt{3}$ alloy.[38] This additional information allows us to make some choices between the possible cyclic and linear products and the alkyne, alkene, and diene functionalities in the desorbed molecules.

3. Results

3.1. Cyclopentane (c-C_5H_{10}). Figure 2 shows TPD spectra from a cyclopentane multilayer (3 ML) film adsorbed on Pt(111) at 100 K that has been subjected to a 50-eV electron exposure of ~2.25 × 10^{14} electrons/cm^2. We monitored many signals, as described above, during TPD following cyclopentane adsorption, including 138 amu for the dimerization of cyclopentyl groups. In the absence of electrons, cyclopentane adsorption on Pt(111) at 100 K is about 80% reversible, and H_2 and cyclopentane were

(35) Tsai, Y.-L.; Xu, C.; Koel, B. E. *Surf. Sci.* **1997**, *385*, 37.
(36) Tsai, Y.-L.; Koel, B. E. *J. Phys. Chem.* **1997**, *B101*, 2895.
(37) Peck, J. W.; Koel, B. E. *J. Am. Chem. Soc.* **1996**, *118*, 2708.
(38) Xu, C.; Peck, J. W.; Koel, B. E. *J. Am. Chem. Soc.* **1993**, *115*, 751.

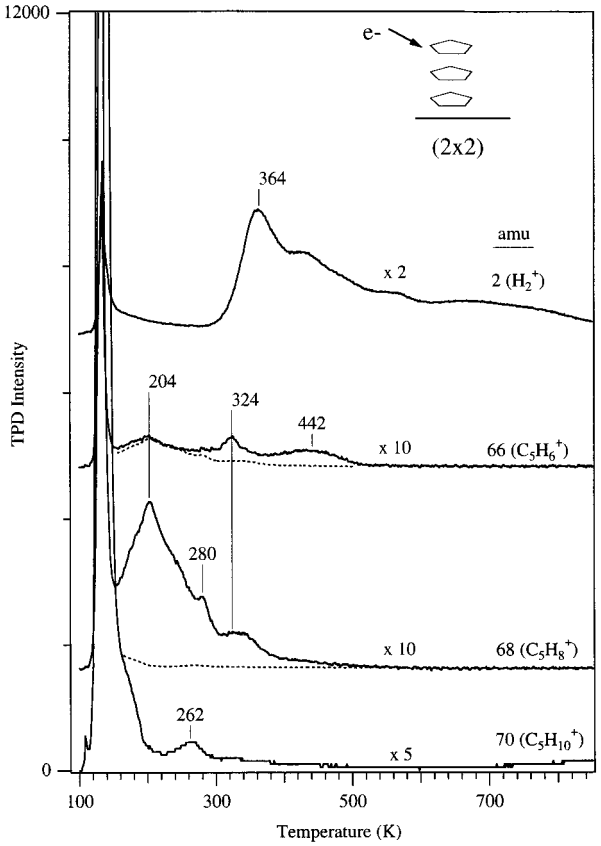

Figure 3. TPD spectra after EID of a 3-ML cyclopentane (c-C_5H_{10}) film on the (2×2) alloy at 100 K.

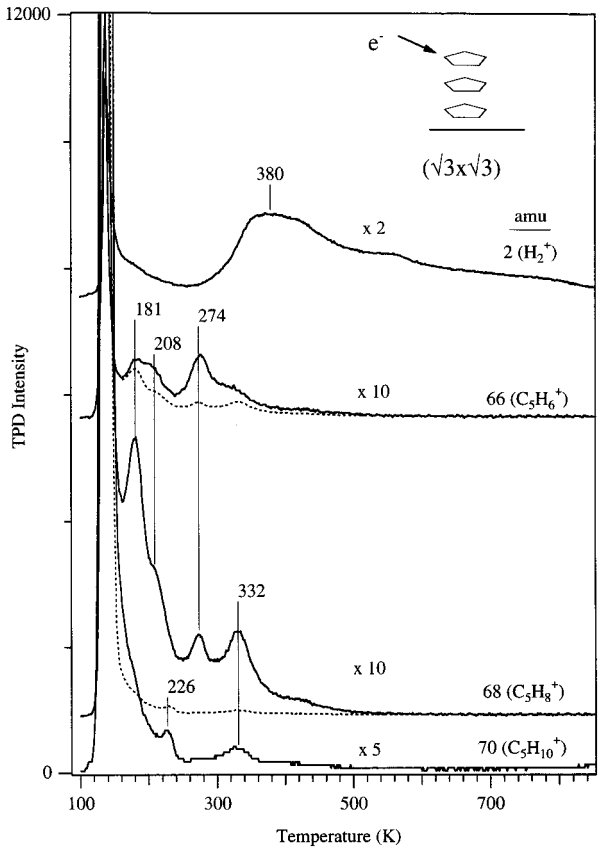

Figure 4. TPD spectra after EID of a 3-ML cyclopentane (c-C_5H_{10}) film on the √3 alloy at 100 K.

the only products observed in TPD.[30] H_2 TPD shows a main peak at 345 K along with two small peaks at 448 and 528 K and a shoulder to 700 K. Adsorbed cyclopentane desorbs molecularly in a peak at 202 K. The C/Pt ratio in AES was 0.05 after these TPD experiments, indicating only a small amount of cyclopentane dehydrogenation, which is consistent with the TPD results.

Following EID of the multilayer, Figure 2 shows that desorption of cyclopentane (c-C_5H_{10}) at 202 K from the monolayer was mostly eliminated due to displacement of adsorbed cyclopentane from the monolayer into the multilayer by the cyclopentyl species formed in EID,[29] while cyclopentane from the multilayer phase desorbs at 134 K. Hydrogenation of cyclopentyl species leads to a small cyclopentane peak at 262 K with a yield of 0.5% of the amount of the cyclopentane monolayer. The primary desorption product observed in TPD was H_2, with some unsaturated hydrocarbons giving rise to the signals for C_5H_8 and C_5H_6. The H_2 yield from thermal decomposition of cyclopentyl is much larger than that from cyclopentane on Pt(111). H_2 desorbs in a peak at 310 K with a broad shoulder extending to 800 K from the complete dehydrogenation of surface hydrocarbon fragments during TPD. We assign the major hydrocarbon product as cyclopentene (c-C_5H_8), desorbing in two adjacent peaks at 213 and 262 K, and the peak at 464 K to some cyclopentadiene (c-C_5H_6) desorption. The peaks at 213 and 262 K in the C_5H_6 spectra appear to be cracking fragments of C_5H_8. LEED showed no extra spots other than the (1×1) structure at any temperature in these experiments.

On the (2×2) alloy, without electrons, nearly all (98%) of the cyclopentane monolayer desorbs molecularly in a peak at 180 K.[31] The main dehydrogenation product, cyclopentene (c-C_5H_8), desorbs in a peak at 280 K. As shown in Figure 3, following EID of the cyclopentane multilayer, cyclopentyl decomposition leads to H_2 desorption in a peak at 364 K with a shoulder extending to 850 K. This increase in the temperature required to completely dehydrogenate the adsorbed hydrocarbon fragment layer illustrates the low dehydrogenation activity of the alloys compared to Pt(111). The principle hydrocarbon products desorbing from this surface are assigned to cyclopentene (c-C_5H_8) at 204 K and cyclopentadiene (c-C_5H_6) at 324 K, in amounts similar to those on Pt(111) but in peaks shifted to lower temperatures. A small amount of hydrogenation leads to cyclopentane desorption at 262 K. No new LEED spots appeared during annealing to 850 K.

Cyclopentane adsorption on the √3 alloy is completely reversible, and cyclopentane desorbs from the monolayer in a peak at 170 K.[31] TPD spectra for cyclopentyl decomposition on the √3 alloy are given in Figure 4. Less H_2 desorption occurs from this surface compared to the other two, and AES detected *no surface carbon* after these TPD experiments. The only signals for separate hydrocarbon products desorbed from the surface were for C_5H_{10}, C_5H_8, and C_5H_6. Hydrogenation of cyclopentyl leads to cyclopentane desorption at 226 and 332 K. A larger C_5H_8 signal was seen from the √3 alloy than from the other two surfaces, with three peaks seen at 181, 274, and 332 K, and the large peak at 181 K is attributed to cyclopentene. The C_5H_6 signal also has multiple peaks at 181, 208, 274 K and a shoulder at 332 K. Some contribution from the cracking of the C_5H_8 product to the C_5H_6 TPD signal occurs (as shown in the dashed line); however, the peak at 274 K is clearly not due to cracking and is assigned to cyclopentadiene (c-C_5H_6) desorption. Some extra spots in addition to the (√3×√3)R30° pattern in LEED were seen at temperatures below 120 K, but no investigation of this structure has been made yet.

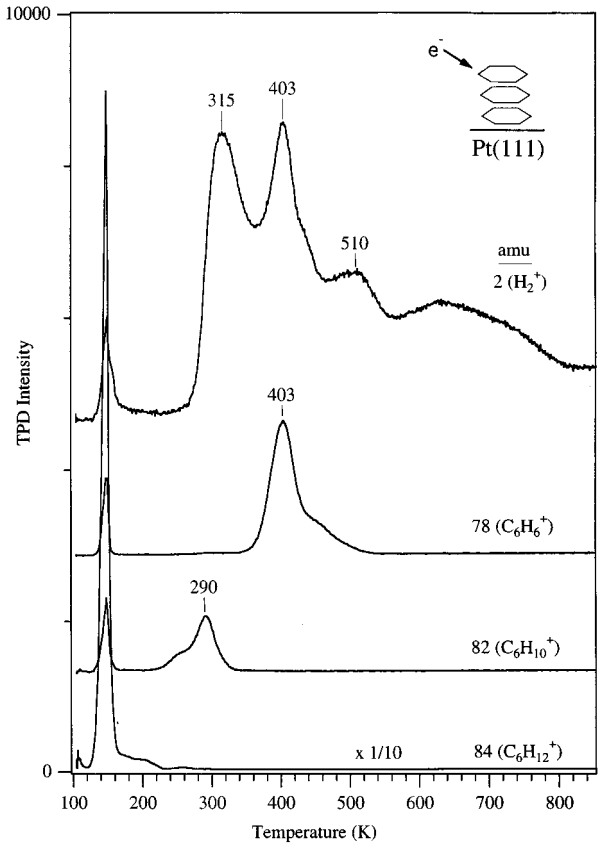

Figure 5. TPD spectra after EID of a 3-ML cyclohexane (c-C_6H_{12}) film on Pt(111) at 100 K.

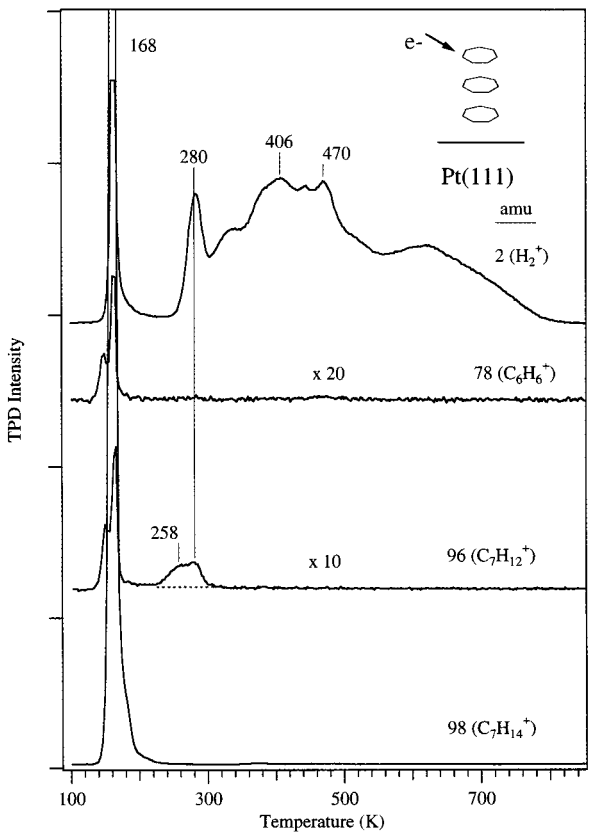

Figure 6. TPD spectra after EID of a 3-ML cycloheptane (c-C_7H_{14}) film on Pt(111) at 100 K.

The multiple desorption peaks on the alloys indicate a complicated set of surface reactions, leading to several different reaction-rate-limited processes for cyclopentene and cyclopentadiene evolution in addition to desorption rate-limited peaks and possibly the desorption of other unsaturated hydrocarbons that could be formed from ring-opening reactions. Because it seems unlikely that ring-opening reactions occur more readily on the $\sqrt{3}$ alloy, we interpret the shift of hydrocarbon product desorption to higher temperatures to indicate the increased stability of cyclopentyl intermediates that arises from a decreased dehydrogenation activity of the alloys. This issue of the multiple desorption peak and the increased stability of cyclopentyl is pertinent to the behavior of the other cycloalkyl intermediates discussed below, and we will see very similar features in the following desorption spectra.

3.2. Cyclohexane (c-C_6H_{12}). Cyclohexane adsorption on Pt(111) has been investigated by many groups,[1,2,28,39−50] giving a pretty clear picture of this chemistry. Cyclohexane is H-bonded to the surface with an adsorption energy of about 14 kcal/mol, and about 50% of the chemisorbed monolayer desorbs at 230 K. Dehydrogenation begins at 180−195 K, corresponding to an activation barrier of 13.4 kcal/mol, and takes place via cyclohexene (c-C_6H_{10}) to form adsorbed benzene. No significant gas-phase cyclohexene or benzene is observed during TPD because of efficient dehydrogenation of these adsorbates. No other intermediates have been identified on Pt(111), although a cycloallylic (c-C_6H_9) species has been predicted[28,39] and inferred from determination of the C/H stoichiometry of the adlayer following heating,[47,50] and cyclohexadiene dehydrogenation yields benzene.[37]

Figure 5 shows results from electron activation of cyclohexane multilayers on Pt(111).[29] The cyclohexane monolayer peak at 228 K has been eliminated by displacement of cyclohexane from the monolayer by cyclohexyl species, and the cyclohexane peak at 254 K arises from a small amount of hydrogenation of cyclohexyl during TPD. Compared to cyclohexane thermal chemistry in the absence of electrons, Figure 5 shows much more H_2 desorption and the new products cyclohexene and benzene. The increased yield of these two hydrocarbon products from cyclohexyl decomposition compared to that from cyclohexane is a coverage effect (because half of the cyclohexane desorbs) resulting from poisoning of the surface by a larger concentration of cyclohexyl-derived surface species. For comparison, cyclohexene[51] and cyclohexadiene[37] adsorption and reaction produce benzene desorption in TPD.

We have previously reported on studies of cyclohexane adsorption on the two alloy surfaces[28] and also on EID

(39) Gland, J. L.; Baron, K.; Somorjai, G. A. *J. Catal.* **1975**, *36*, 305.
(40) Firment, L. E.; Somorjai, G. A. *J. Chem. Phys.* **1977**, *66*, 2901.
(41) Demuth, J. E.; Ibach, H.; Lehwald, S. *Phys. Rev. Lett.* **1978**, *40*, 1044.
(42) Tsai, M. C.; Friend, C. M.; Mutterties, E. L. *J. Am. Chem. Soc.* **1982**, *104*, 2539.
(43) Stohr, J.; Sette, F.; Johnson, A. L. *Phys. Rev. Lett.* **1984**, *53*, 1684.
(44) Kang, D. B.; Anderson, A. B. *J. Am. Chem. Soc.* **1985**, *107*, 7858.
(45) Hitchcock, A. P.; Newbury, D. C.; Ishii, I.; Stohr, J.; Horsley, J. A.; Redwing, R. D.; Johnson, A. L.; Sette, F. L. *J. Chem. Phys.* **1986**, *85*, 4849.
(46) Land, D. P.; Pettiette-Hall, C. L.; Mclver, R. C., Jr.; Hemminger, J. C. *J. Am. Chem. Soc.* **1989**, *111*, 5970.
(47) Rodriguez, J. A.; Campbell, C. T. *J. Phys. Chem.* **1989**, *93*, 826.
(48) Pettiette-Hall, C. L.; Land, D. P.; Mclver, R. C., Jr.; Hemminger, J. C. *J. Am. Chem. Soc.* **1991**, *113*, 2755.
(49) Parker, D. H.; Pettiette-Hall, C. L.; Li, Y. Z.; Mclver, R. C., Jr.; Hemminger, J. C. *J. Phys. Chem.* **1992**, *96*, 1888.
(50) Bussell, M. E.; Henn, F. C.; Campbell, C. T. *J. Phys. Chem.* **1992**, *96*, 5978.
(51) Xu, C.; Koel, B. E. *Surf. Sci.* **1994**, *304*, 249.

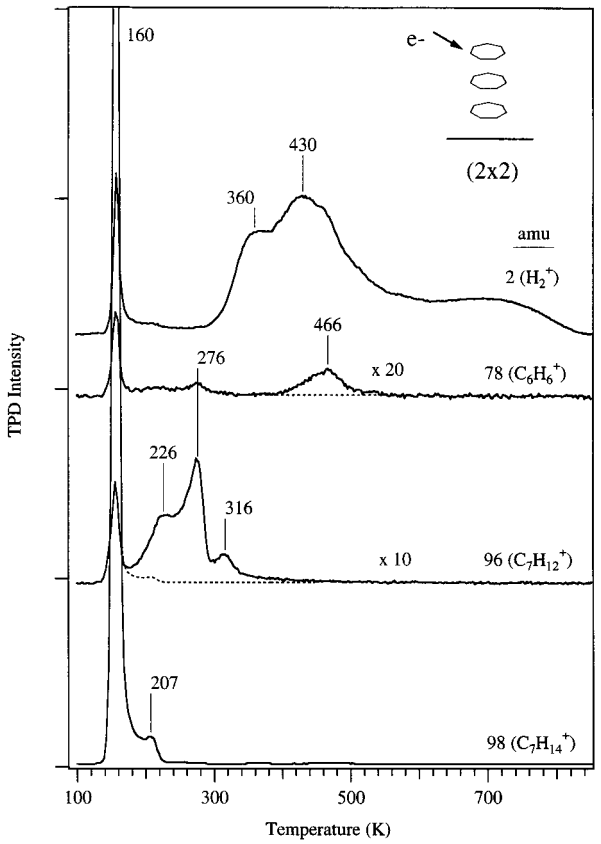

Figure 7. TPD spectra after EID of a 3-ML cycloheptane (c-C_7H_{14}) film on the (2×2) alloy at 100 K.

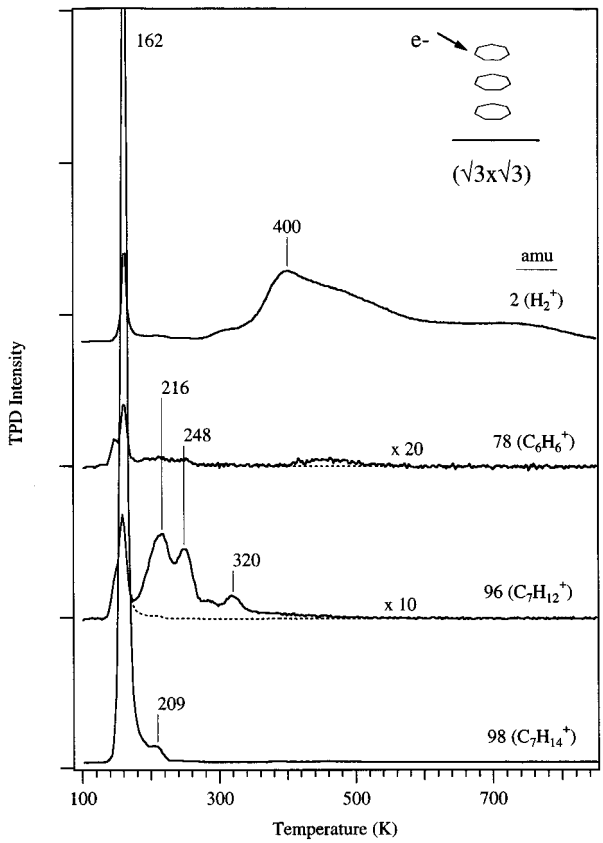

Figure 8. TPD spectra after EID of a 3-ML cycloheptane (c-C_7H_{14}) film on the √3 alloy at 100 K.

experiments activating cyclohexane multilayers on these surfaces.[27,28] For brevity, we will not reproduce those results here, but we will compare the data to those for Pt(111) and the other cycloalkyl results in the Discussion section. Cyclohexane adsorption on the two alloys without electron activation is completely reversible; no decomposition and no H_2 desorption occurs in TPD.[28] Cyclohexane desorption peaks were seen at 194 and 185 K on the (2×2) and √3 alloys, respectively, indicating adsorption energies of 11.7 and 11 kcal/mol, respectively. Thermal decomposition of cyclohexyl produced by EID led to desorption of benzene and cyclohexene on these substrates, with the amount of carbon buildup and relative yields of the two hydrocarbon products varying with Sn concentration in the surface layer.[28] Cyclohexadiene desorption was not observed, in contrast to that of cyclopentadiene discussed above, but this is consistent with our finding that 1,3-cyclohexadiene is converted completely to benzene on both alloys.[37]

3.3. Cycloheptane (c-C_7H_{14}). Adsorption of cycloheptane gives rise to molecular desorption peaks in TPD at 248, 209, and 207 K on Pt(111)[30] and the (2×2) and √3 alloys,[31] respectively. While similar coverages in the chemisorbed monolayer are obtained on the three surfaces, the extent of decomposition varies from 20% to 7% and 0% on Pt(111)[30] and the (2×2) and √3 alloys,[31] respectively. Thus, cycloheptane is largely reversibly adsorbed on Pt(111) and completely reversibly adsorbed on the √3 alloy. No other desorption products from these surfaces were seen in TPD without electron activation, except for a small peak at 268 K for 96 (C_7H_{12}) amu on the √3 alloy. In all of the following EID-based experiments, we monitored signals from all three surfaces during TPD at 92 (toluene, C_7H_8); 94, 96, 98 (C_7H_x); and 100 (C_7H_{16}, *n*-heptane) amu.

Figure 6 shows TPD results for cycloheptyl decomposition on Pt(111). Much more H_2 desorbs than the amount from cycloheptane decomposition, and TPD shows a peak at 280 K with a broad, structured evolution up to 800 K. Cycloheptene (c-C_7H_{12}) is the only hydrocarbon product desorbed, and it evolves in two closely spaced peaks at 258 and 280 K. No desorption of cycloheptane was seen from the monolayer at 248 K or from hydrogenation of cycloheptyl. No benzene desorption was detected.

On the (2×2) alloy, as presented in Figure 7, a small amount of the adsorbed cycloheptane not eliminated by the electron dosing in EID desorbs at 207 K. Surface cycloheptyl species produced by EID undergo further dehydrogenation to form surface carbon and desorb H_2. H_2 desorbs in peaks at 360 and 430 and a plateau near 850 K in much larger amounts compared to that from cycloheptane decomposition on the (2×2) alloy. The main hydrocarbon desorbed from this surface is cycloheptene (c-C_7H_{12}) at 276 K in a larger yield compared to that from Pt(111). Some benzene (C_6H_6) desorption can be detected in a peak at 466 K. This temperature is the same as that for benzene desorption from cyclohexyl dehydrogenation on this alloy[28] and close to that for benzene desorption following benzene adsorption on this alloy.[28]

Figure 8 gives several TPD spectra from cycloheptyl decomposition on the √3 alloy. Cycloheptane desorption from the monolayer is again nearly eliminated by EID production of cycloheptyl species. On the √3 alloy, however, complete dehydrogenation of cycloheptyl intermediates was strongly reduced and this can be seen in the reduction in the amount of H_2 evolution, which occurs in a broad distribution from 260 to 850 K with a peak near 400 K. The only independent hydrocarbon TPD signals from dehydrogenation occur at 96 amu (C_7H_{12}). We assign the main product to be cycloheptene (c-C_7H_{12}), which desorbs in a peak at 216 K. The yields of cycloheptene are

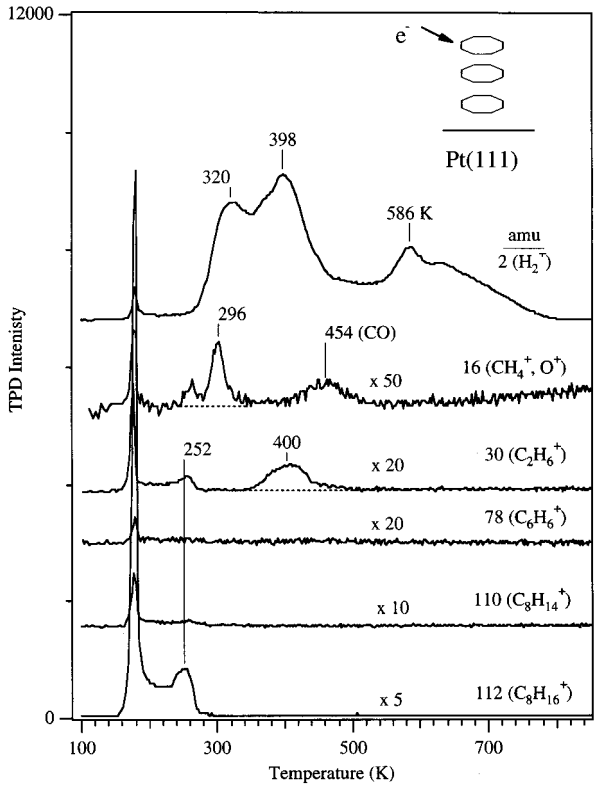

Figure 9. TPD spectra after EID of a 3-ML cyclooctane (c-C_8H_{16}) film on Pt(111) at 100 K.

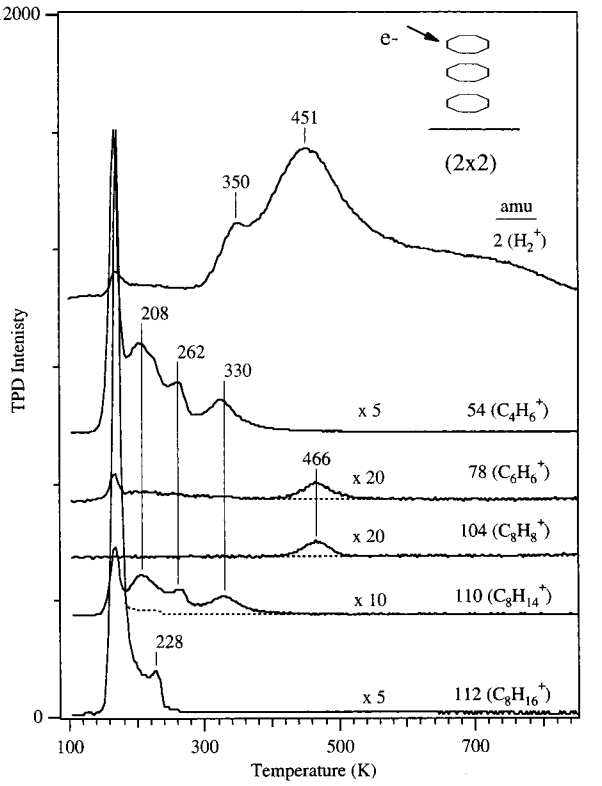

Figure 10. TPD spectra after EID of a 3-ML cyclooctane (c-C_8H_{16}) film on the (2×2) alloy at 100 K.

similar on both surface alloys and much greater than that on Pt(111). C_6H_6 evolution is inhibited on the √3 alloy, as we saw previously for cyclohexyl,[28] and only a trace of C_6H_6 desorption occurs on the √3 alloy. No cycloheptadiene desorption was observed, in contrast to the case for cyclopentadiene discussed earlier.

3.4. Cyclooctane (c-C_8H_{16}). Physisorbed cyclooctane desorbs at 174 K on all three surfaces, and chemisorbed cyclooctane desorbs at 260, 230, and 224 K on Pt(111)[30] and the (2×2) and √3 alloys,[31] respectively. Only 30% of the cyclooctane monolayer decomposes on Pt(111), and H_2 desorption occurs in a large peak at 356 with smaller peaks at 568 and 627 K. No hydrocarbon decomposition products were desorbed, except a trace amount of ethane at 260 and 420 K and methane at 296 K. On the (2×2) alloy, cyclooctane is mostly (94%) reversibly adsorbed, yielding only H_2 desorption and traces of ethane at 280 and 298 K, acetylene at 266 K, and methane at 245 K. Cyclooctane is reversibly adsorbed on the √3 alloy, with essentially no H_2 desorption and only a trace amount of methane at 180 K.

Figure 9 shows TPD spectra of cyclooctyl decomposition on Pt(111). In addition to those listed previously, signals were monitored during TPD from the three surfaces at 82, 86 (C_6H_x); 92 (C_7H_8); 102, 104, 106, 108, 110, 112 (C_8H_x); and 222 (dimerization of cyclooctyl) amu. After EID in the multilayer cyclooctane film, more H_2 desorption and less desorption of cyclooctane from the chemisorbed state were obtained. In a substantial departure from the EID results for the C_{5-7} cycloalkane films, no C_8H_{14} signal that can be attributed to cyclooctene (c-C_8H_{14}) desorption was observed from cyclooctyl decomposition on Pt(111). Also, more ethane is desorbed, but at the same temperature, compared to that for cyclooctane on Pt(111).

TPD spectra for cyclooctyl decomposition on the (2×2) alloy are shown in Figure 10. The desorbed products in TPD are H_2, C_8H_{14}, and C_8H_8. We assign the C_6H_6 and C_4H_6 signals to cracking fragments of larger hydrocarbons. Because of the desorption temperature, it is possible that there is some benzene evolution, but at this point we have no independent evidence for it. H_2 desorbs in broad peaks at 350 and 451 with a tail up to 850 K. The primary unsaturated hydrocarbon product desorbed is assigned to cyclooctene (c-C_8H_{14}), which desorbs primarily at 208 and 262 K. Cyclooctatetraene (c-C_8H_8; COT) desorbs in a peak at 466 K.

On the √3 alloy, as shown in Figure 11, a small amount of cyclooctane molecularly adsorbed in the monolayer can be observed to desorb at 224 K. Cyclooctyl dehydrogenates to yield H_2 and a hydrocarbon product detected at 110 amu (C_8H_{14}), along with a trace amount of benzene at 470 K, as products in TPD. H_2 desorption has a small peak at 288 K and a broad peak at 454 K and extends to 850 K. We attribute the C_8H_{14} curve to cyclooctene (c-C_8H_{14}), which desorbs principally at 208 K, with a total yield comparable to that from the (2×2) alloy. In contrast to the case of the (2×2) alloy, no COT desorption occurred from cyclooctyl dehydrogenation on the √3 alloy.

4. Discussion

Molecular adsorption of cycloalkanes in the C_5-C_8 size range on Pt(111) at 100 K is mostly reversible, and TPD leads to predominately molecular desorption.[30] Thermal decomposition that occurs during TPD gives rise to H_2 desorption and the accumulation of surface carbon, with no other hydrocarbon products desorbed from the surface. Cyclohexane stands out in this series of compounds as being more reactive with the Pt(111) surface, since about 50% of the adsorbed cyclohexane layer decomposes during TPD. On the two Sn/Pt(111) alloy surfaces, adsorption of the C_5-C_8 cycloalkanes is weaker and less decomposition occurs during TPD, especially in the case of the √3 alloy where the amount of decomposition is nearly zero (<1%).[31] Notably, for cyclohexane, no thermal decomposition occurs

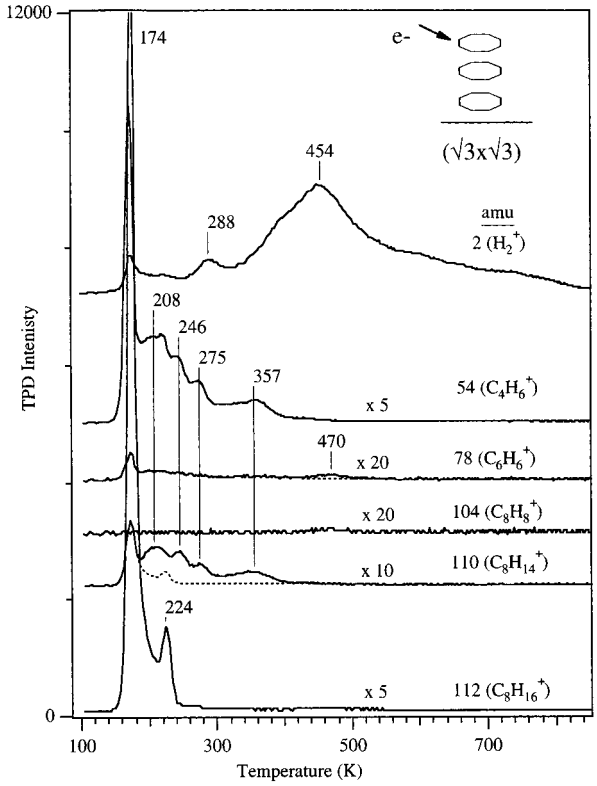

Figure 11. TPD spectra after EID of a 3-ML cyclooctane (c-C_8H_{16}) film on the $\sqrt{3}$ alloy at 100 K.

Table 1. Major Gas Products Observed in TPD Following Cycloalkane Adsorption without and with Electron Activation

		Pt(111)	Sn/Pt(111) surface alloys (2x2)	Sn/Pt(111) surface alloys √3
cyclopentane	no electrons	H_2,	H_2,	H_2,
	EID	H_2,	H_2,	H_2,
cyclohexane [28]	no electrons	H_2,		
	EID	H_2,	H_2,	H_2,
cycloheptane	no electrons	H_2,	H_2,	H_2,
	EID	H_2,	H_2,	H_2,
cyclooctane	no electrons	H_2,	H_2,	H_2,
	EID	H_2, C_2H_6,	H_2,	H_2,

on either alloy surface. Cyclopentane decomposition evolves cyclopentene in TPD from both alloy surfaces, while cycloheptane and cyclooctane decomposition leads to some desorption of the corresponding cycloalkenes on the $\sqrt{3}$ alloy. Table 1 summarizes these results, listing the thermal decomposition products for each molecule on these three surfaces obtained in the absence of electron activation.

Table 1 also provides a list of the principle gaseous products formed in TPD after electron activation via EID of cycloalkane multilayers on Pt(111) and the two Sn/Pt(111) surface alloys. EID of these multilayers, under conditions of an incident electron beam energy of 50 eV and an average electron exposure of 4.5×10^{14} electrons/cm^2, leads to a chemisorbed monolayer containing predominately a single cycloalkyl species corresponding to the fragment produced by cleavage of a single C−H bond in the molecular precursor.[21,27] Overall, thermal decomposition of these cycloalkyl species on Pt(111) leads to some desorption of unsaturated hydrocarbons in TPD, except for cyclooctyl decomposition, which does not. This change from the chemistry of the cycloalkane adlayer arises simply because of the increased concentration of surface-bound hydrocarbons, evidenced by a larger H_2 yield in TPD and C/Pt ratio in AES following TPD, which blocks sites and increases the barrier for decomposition of some of the intermediates. The thermal decomposition of cycloalkyl intermediates on the two Pt−Sn alloys always leads to a higher desorption yield of unsaturated hydrocarbons and lower amounts of H_2 in TPD compared to Pt(111). Also some selectivity for the various products results from different Sn concentrations in the surface alloy. Now, we will try to summarize the overarching aspects of all of this chemistry.

TPD spectra after formation of the cyclopentyl monolayer show cyclopentane, cyclopentene, cyclopentadiene, and H_2 evolution on all three surfaces. Hydrogenation of cyclopentyl to produce cyclopentane occurs at the same temperature of 262 K on Pt(111) and the (2×2) alloy but takes place in two different processes at 226 and 332 K on the $\sqrt{3}$ alloy. H_2 desorption decreases in amount, and the temperature profile shifts. The onset for H_2 desorption, and the highest temperature for H_2 evolution, shifts ∼50 K to higher temperatures as Sn is added to the surface. Figure 12 compares the TPD spectra of the two hydrocarbon products from cyclopentyl decomposition on all three surfaces: (a) cyclopentene (c-C_5H_8) and (b) cyclopentadiene (c-C_5H_6). The cyclopentene yields are similar on the three surfaces but have quite different desorption temperatures and profiles. Cyclopentene desorbs in two states at 213 and 262 K on Pt(111), probably due to two adsorption sites. Avery[52] observed a single peak at 285 K for cyclopentene desorption from cyclopentene adsorption on Pt(111). The cyclopentene peak is shifted to lower temperatures upon alloying with Sn, to 204 K on the (2×2) alloy, and to 181 K on the $\sqrt{3}$ alloy. This indicates a weakening of the bonding of cyclopentene to the alloy surfaces, similar to that for ethylene,[35,53] propylene,[35] butenes,[36] and cyclohexene,[51] but maintenance of a reasonable activity for cyclopentyl decomposition. The high-temperature cyclopentene peaks at 274 and 332 K arise from hydrogenation of some other intermediate at these temperatures.

As seen in Figure 12b, cyclopentene can be dehydrogenated on all three surfaces. Some cyclopentadiene (c-C_5H_6) desorption is seen for Pt(111) at 464 K, but the amount of cyclopentadiene desorption increases with increasing Sn concentration. On the (2×2) alloy, a peak occurs at 325 with a broad feature at 435 K, and on the $\sqrt{3}$ alloy, desorption occurs from 180 to 350 K with a peak at 276 K. Some contribution of cyclopentene cracking in the QMS contributes to the cyclopentadiene TPD intensity, and we have indicated this by the dashed line in the spectra. The cyclopentadiene desorption temperature decreases with increasing surface Sn concentration. We assign the 464 K peak on Pt(111) to a desorption rate-

(52) Avery, N. R. *Surf. Sci.* **1984**, *137*, L109.
(53) Paffett, M. T.; Gebhard, S. C.; Windham, R. G.; Koel, B. E. *Surf. Sci.* **1989**, *223*, 449.

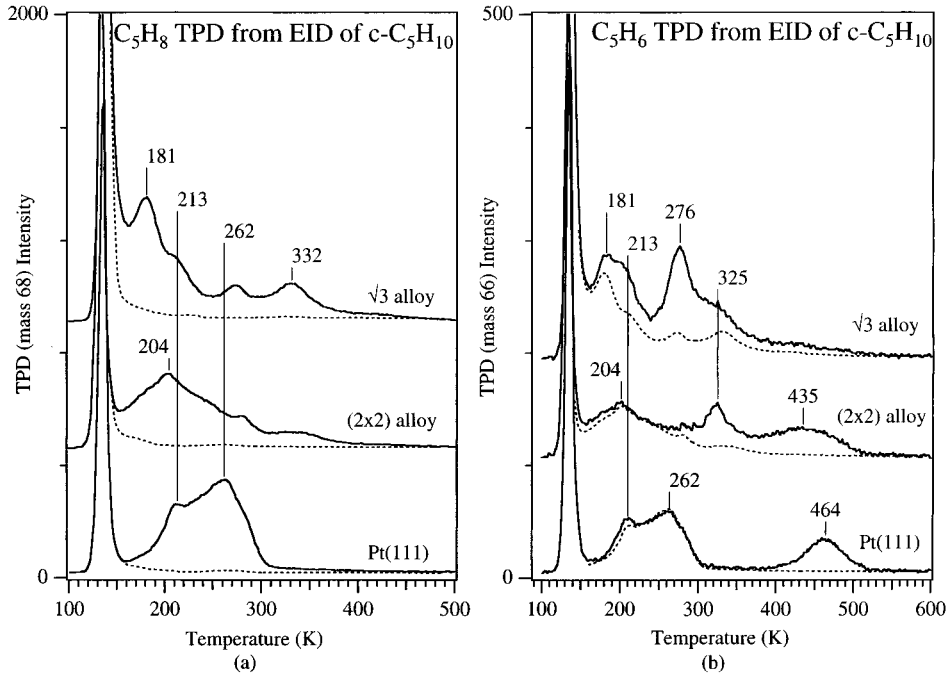

Figure 12. Comparison of hydrocarbon TPD spectra after EID of cyclopentane (c-C_5H_{10}) films on Pt(111) and Pt−Sn surface alloys at 100 K: (a) cyclopentene (c-C_5H_8); (b) cyclopentadiene (c-C_5H_6).

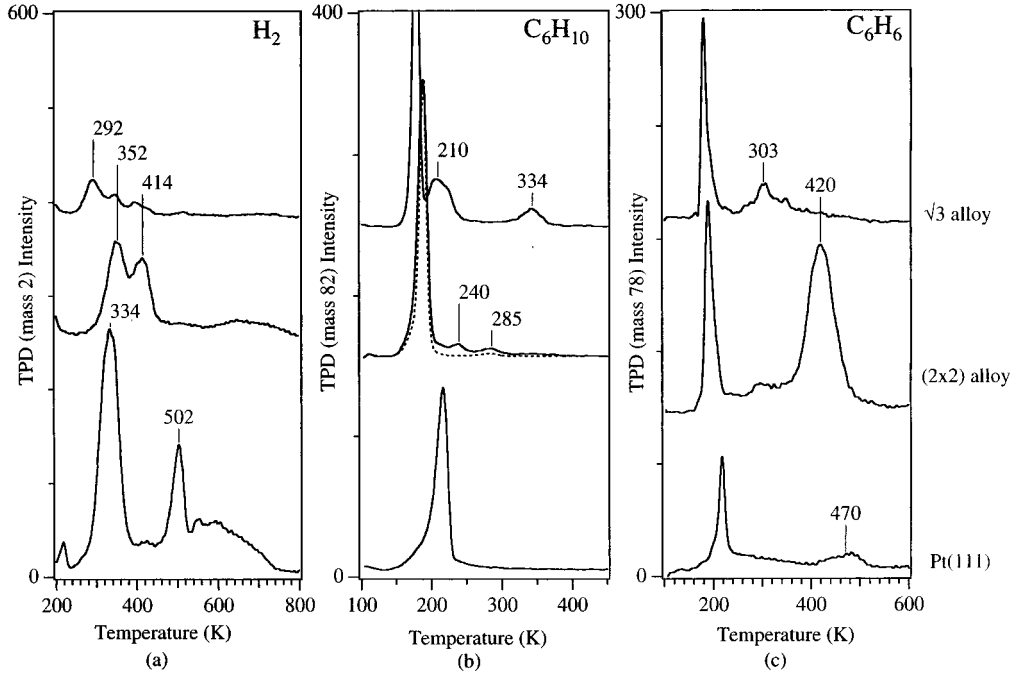

Figure 13. Comparison of TPD spectra after EID of cyclohexane (c-C_6H_{12}) films on Pt(111) and Pt−Sn surface alloys at 100 K: (a) hydrogen (H_2); (b) cyclohexene (c-C_6H_{10}); (c) benzene (C_6H_6).

limited process corresponding to a desorption activation energy of about 29 kcal/mol for adsorbed cyclopentadiene. Adding Sn to the surface weakens the bonding of cyclopentadiene and produces peaks at 325 and 213 or 276 K on the (2×2) and √3 alloys, respectively. The higher yield of cyclopentadiene on the two alloys could be due to this weaker bonding and/or a higher activation barrier for dehydrogenation of cyclopentadiene on the surface.

Cyclohexyl decomposition leads to H_2, cyclohexene, and benzene products in TPD spectra on all three surfaces.[28] Figure 13 reproduces some of these data, so that comparisons can be made to the other cycloalkyl results. The conditions for preparing the initial cyclohexyl layers in these experiments led to less than saturation coverage of cyclohexyl species on the surfaces. (This was done to emphasize the selectivity for benzene formation in our former work.[28]) However, the reactivity and selectivity trends upon alloying are relevant. As shown in Figure 13a, the total amount of H_2 desorption and surface carbon following TPD decreases with increasing Sn. At this low coverage, the Pt(111) surface mostly dehydrogenates cyclohexyl all the way to carbon, showing no cyclohexene (c-C_6H_{10}) desorption in Figure 13b and only a small benzene (C_6H_6) yield in Figure 13c. The H_2 peak at 334 K is an H_2 desorption rate-limited peak due to cyclohexyl to benzene conversion, and the peak and features above 502 K are characteristic of benzene decomposition on Pt(111). The (2×2) alloy produces much less H_2 in TPD,

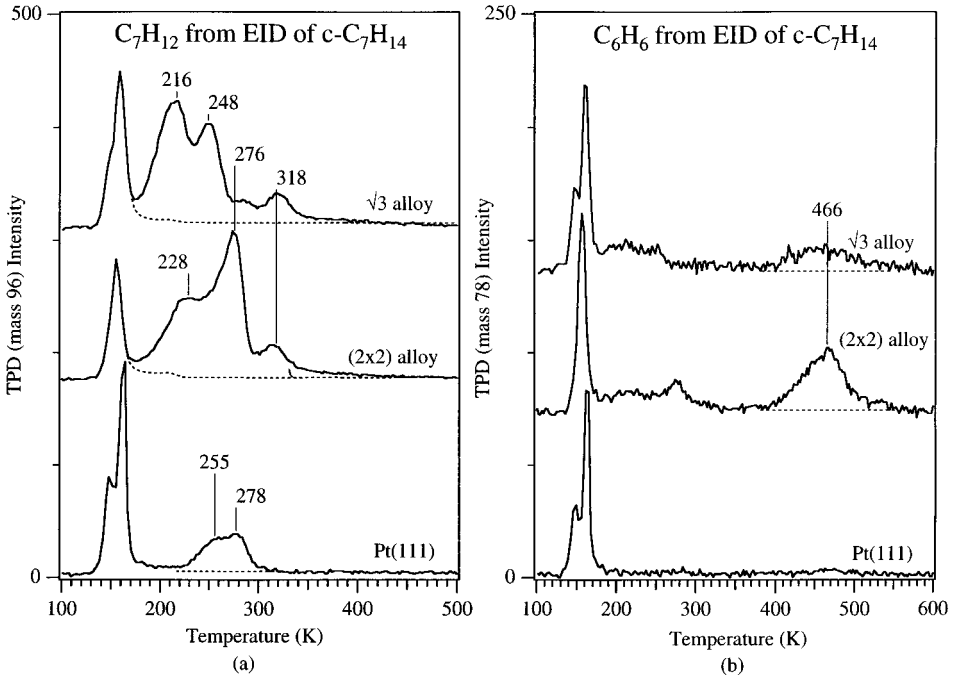

Figure 14. Comparison of hydrocarbon TPD spectra after EID of cycloheptane (c-C_7H_{14}) films on Pt(111) and Pt−Sn surface alloys at 100 K: (a) cycloheptene (c-C_7H_{12}); (b) benzene (C_6H_6).

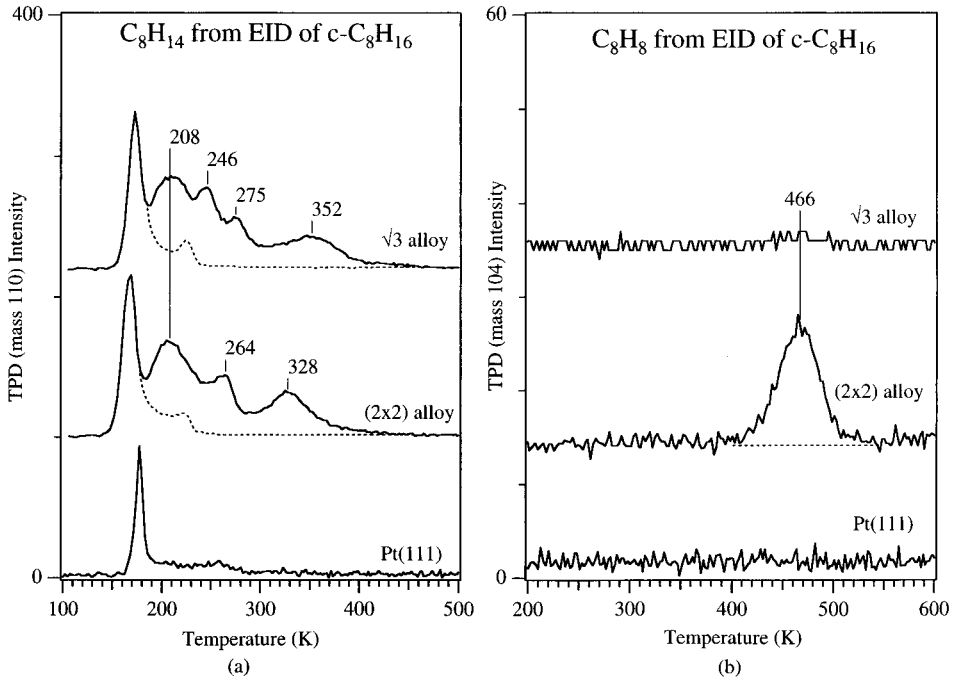

Figure 15. Comparison of hydrocarbon TPD spectra after EID of cyclooctane (c-C_8H_{16}) films on Pt(111) and Pt−Sn surface alloys at 100 K: (a) cyclooctene (c-C_8H_{14}); (b) benzene (C_6H_6).

and importantly the high-temperature peak at 502 K from benzene decomposition is absent. We suggest that the peak at 352 K is from dehydrogenation of cyclohexyl to a cycloallylic (c-C_6H_9) intermediate and that the peak at 414 K is primarily from dehydrogenation of the c-C_6H_9 species to benzene. This illustrates a much lower reactivity of the (2×2) alloy compared to Pt(111) for dehydrogenation of the c-C_6H_9 intermediate. A small amount of cyclohexene desorbs in two peaks at 240 and 285 K, as shown in Figure 13b, with the low-temperature peak due to a desorption rate-limited process[51] and the high-temperature peak due to hydrogenation of some intermediate. As shown in Figure 13c, the (2×2) alloy desorbs a considerable amount of gas-phase benzene product, in a peak at 420 K. Cyclohexyl decomposition on the $\sqrt{3}$ alloy leads to very little H_2 and benzene and mostly to cyclohexene desorption. Here, two cyclohexene peaks occur at 210 and 334 K. The low-temperature peak is due to a desorption rate-limited process,[51] while the higher temperature evolution must be from hydrogenation of some intermediate. The higher yield of cyclohexene compared to benzene indicates that the $\sqrt{3}$ alloy is not sufficiently reactive to dehydrogenate cyclohexene to form other intermediates that lead to benzene. The high selectivity of the (2×2) alloy for benzene arises from a tailoring of the reactivity of the surface—sufficient reactivity to dehydrogenate cyclohexene and the c-C_6H_9

intermediate but insufficient reactivity to dehydrogenate the benzene product.

Parts a and b of Figure 14 show the cycloheptene (c-C_7H_{12}) and benzene (C_6H_6) formations, respectively, from cycloheptyl decomposition on these three surfaces. Much more cycloheptene is formed and desorbs at lower temperatures, on the two surface alloys compared to Pt(111). On the basis of our previous studies of cyclohexene[51] adsorption and desorption on these three surfaces, we assign the desorption of cycloheptene at 255 and 278 K on Pt(111) to desorption rate-limited evolution from two adsorption sites and the cycloheptene peaks at 228 K on the (2×2) alloy and 216 K on the $\sqrt{3}$ alloy to desorption rate-limited processes. This is consistent with the general weakening of the bonding of alkenes to the alloy surfaces but maintenance of a reasonable activity for cycloheptyl decomposition. The higher temperature cycloheptene peaks on the alloys evidently arise from hydrogenation of some other intermediate at these temperatures. Notably, no cycloheptadiene (c-C_7H_{10}) desorption was seen for any of these surfaces, but we note that no cyclohexadiene desorption occurs either when cyclohexadiene is adsorbed on these three surfaces because of an efficient conversion to benzene.[37] In Figure 14b, the right panel shows the small amount of gas-phase C_6H_6 evolution that occurs, with the (2×2) alloy having the highest yield and no benzene evolved from the Pt(111) surface. The desorption temperature of 466 K for benzene from the (2×2) alloy is that expected for low coverages of benzene formation from cyclohexyl as well as desorption of benzene after benzene adsorption on the (2×2) alloy.[28] Ring reduction reactions evidently do not occur readily on the alloys, since benzene is reversibly adsorbed and would appear if produced in substantial quantity.

In Figure 15, c-C_8H_{14} (cyclooctene, or possibly pentalane[54]) and C_8H_8 (cyclooctatetraene, COT) TPD spectra are shown for cyclooctyl decomposition on the three surfaces. In contrast to that for all of the other cycloalkanes, no cycloalkene desorption was observed on the Pt(111) surface. C_8H_{14} desorbs at similar temperatures and in nearly the same amounts on the two Pt−Sn alloys, with the peaks near 208 K most likely corresponding to desorption rate-limited processes. The higher temperature cyclooctene peaks on the alloys are generally in the same temperature range as those for the smaller cycloalkenes and arise from hydrogenation of hydrocarbon intermediates at these temperatures. As shown in Figure 15b, a very small amount of cyclooctatetraene (COT) desorption occurred at 466 K on the (2×2) alloy only. No cyclooctadiene (COD) or benzene evolution was observed on any of the surfaces.

Activation of these cycloalkane multilayers to produce adsorbed monolayers of primarily cycloalkyl species has contributed to an improved picture of the reactivity and hydrocarbon chemistry on Pt−Sn alloys. Obviously, these data represent only a cursory examination of this interesting chemistry. We are planning a number of spectroscopic studies and detailed kinetics measurements. However, several important aspects of this chemistry emerge. Cycloalkyl thermal decomposition on the two surface alloys studied always leads to higher yields of cycloalkenes and decreased carbon buildup compared to the case on Pt(111). The origin of this increase in cycloalkene yield is not clear, because it could arise from a lower cycloalkene adsorption energy or a higher barrier to cycloalkene dehydrogenation. The reactivity of the Pt−Sn alloys is clearly reduced, that is, reversibly adsorbing ethylene,[35,53] other alkenes,[35,36,51] and benzene,[28] but all of these surfaces dehydrogenate cycloalkyl species rather easily. There is no appreciable evolution in TPD of small hydrocarbon products (methane, ethane, ethylene, etc.) that would be formed by C−C bond breaking on any of these surfaces under our conditions. This is expected behavior even though the barriers to dehydrogenation increase, because C−C bond cleavage is generally regarded as more structure sensitive, requiring a larger ensemble size, than C−H bond breaking. However, we did detect some benzene desorption from thermal decomposition of cycloheptyl. Consistent with our earlier studies of cyclohexyl[28] and low coverages of cyclohexene,[51] the (2×2) alloy showed the highest selectivity for gas-phase benzene production. No C−C bond coupling reactions to give dimers of the cycloalkyl species were ever seen, and no toluene desorption was observed for the C_7 and C_8 reactions. Even though the (2×2) alloy quantitatively dehydrogenates 1,3-cyclohexadiene to benzene,[37] we observed some cyclooctatetraene desorption following cyclooctyl decomposition.

5. Conclusion

To further probe the changes that occur in hydrocarbon reactions on Pt(111) surfaces upon alloying with Sn, we have utilized low-energy (50-eV) EID of multilayer cycloalkanes (C_5−C_8) to activate these molecules, producing primarily adsorbed cycloalkyl species, for subsequent thermal decomposition reactions. This survey of the reactivity of a homologous series of cycloalkyls was carried out on a Pt(111) surface and two ordered Pt−Sn alloys, the p(2×2)Sn/Pt(111) and ($\sqrt{3}\times\sqrt{3}$)R30°Sn/Pt(111) surface alloys. Generally, dehydrogenation of cycloalkyl intermediates proceeds easily at low temperatures on all three surfaces. Alloying Sn into the Pt(111) surface layer increases the yield of cycloalkenes and decreases the amount of H_2 desorption, that is, lowering the amount of surface carbon accumulated on the surface after heating to 850 K, compared to that from Pt(111). A lowering of the desorption temperatures of all of the cycloalkenes accompanies this higher selectivity, with the largest effect seen on the $\sqrt{3}$ alloy, which does not contain any pure Pt 3-fold sites. Some benzene desorption was observed for c-C_{6-7} on the (2×2) alloy.

Acknowledgment. We thank the donors of the Petroleum Research Fund, administered by the American Chemical Society, for support of this work.

LA970711J

(54) Pines, H. *The Chemistry of Catalytic Hydrocarbon Conversions*; Academic Press: New York, 1981; Chapter 4.